BULGARIAN ACADEMY OF SCIENCES

CYBERNETICS AND INFORMATION TECHNOLOGIES • Volume **9**, No 3

Sofia • 2009

Multiple Signal Extraction in Jamming Using Adaptive Beamforming with Arbitrary Array Configurations

Vera Behar[1], *Christo Kabakchiev*[2]

[1]*Institute for Parallel Processing, 1113 Sofia*
E-mail: behar@bas.bg
[2] *University of Sofia "St. Kliment Ohridski", 1164 Sofia*
E-mail: ckabakchiev@fmi.uni-sofia.bg

Abstract: *In this paper, the performance of the two beamforming methods, conventional and MVDR QR-based, are used for multiple signal extraction under conditions of jamming using three various array configurations. The quality of source localization under conditions of strong broadband interference is evaluated in terms of the following quality measures estimated at the beamformer output – the angular resolution of signals, the peak sidelobe level and the signal-to-interference-plus-noise ratio (SINR) improvement. The simulation results demonstrate the better and more stable angular resolution of signals, provided by the MVDR method, compared to the conventional beamforming method.*

Keywords: *Source localization, digital beamforming, adaptive array processing, broadband interference suppression.*

1. Introduction

Extraction of the time-domain signals incoming from desired directions is an important problem in many applications – radar, sonar, communications, and others. Different beamforming methods can be used for signal extraction by rotating the central beam of an array to give maximum received signal strength [1, 5]. The conventional and non-adaptive beamforming method is known as the delay-and-sum beamformer. It is the simplest method, according to which the array weights of equal magnitudes and the different phases are selected to steer the array in the desired direction [1, 2]. This beamformer has unity response in each look direction, that is, the mean output power of the beamformer in the look direction is the same as the source power. Under conditions of no directional interferences, this beamformer provides maximum SNR, but it is not effective in the presence of directional interference, intentional or unintentional. The other beamforming methods, such as an adaptive Minimum Variance Distortionless Response (MVDR) method can overcome this problem by suppressing interfering signals from off-axis directions [3, 4, 5]. By steering the array, the MVDR-beamformer adaptively calculates the array weights that provide the maximum gain in all directions of concern while minimizing the power in the other (interference) directions. To suppress jamming signals, this beamformer does not require the apriori information about them. It requires only information about the direction-of-arrival of the desired signal.

The online updating of the array weights by the MVDR method requires the online estimation and inversion of the sample covariance matrix. In many practical applications, it is very expensive computationally and may be very unstable if the sample covariance matrix is ill-conditioned. However, a numerical stable and computationally efficient algorithm (*QR*-based) can be obtained by using *QR*-decomposition of the incoming signal matrix [4].

In this paper, the performance of the two beamformers, conventional and MVDR QR-based, that operate under conditions of jamming, is evaluated for three basic array configurations (linear, rectangular circular). The capability of each beamformer to extract multiple signals arrived from different directions is evaluated in terms of three quality measures, which are estimated at the beamformer output. They are the angular resolution, the peak sidelobe level and the improvement in SINR.

2. Signal model

The signal model is based on the scenario, according to which one or several (N) desired signals combined with the wideband interference arrive at the antenna array input. The complex vector of array observations at time instant k can be modeled as

$$x(k) = \sum_{n=1}^{N} a_{c,n} s_n(k) + bj(k) + n(k)\,, \tag{1}$$

where $a_{c,n}$ is the M-element array response vector of in the n-th signal direction, b is the M-element array response vector in the jammer direction, $s(k)$ and $j(k)$ are the complex samples of the signal and interference, respectively, and finally, $n(k)$ is the M-element vector of an Additive White Gaussian Noise (AWGN).

3. Conventional beamforming method

The object of beamforming is to increase the gain of the antenna array in the signal direction and decrease the gain in the other directions. The output of a narrowband array with M antenna elements is formed as

(2) $$y(k) = W^{\mathrm{H}} x(k)\,,$$

where k is the time instant, and $x(k)$ is the complex vector of array observations, $W=[w_1, w_2,\ldots, w_M]^{\mathrm{T}}$ is the complex vector of the beamformer weights, T and H denote transpose and conjugate transpose, respectively. In the conventional "sum-and-delay" beamformer, the complex vector of weights W is equal to the array response vector a_{c}, which is determined by an array configuration:

(3) $$W_{\mathrm{conv}} = a_{\mathrm{c}}\,.$$

4. MVDR beamforming method

Let us assume that the vector a_{c} represents the direction of arrival of the desired signal. The optimal weight vector W can be chosen to maximize the Signal-to-Interference-plus-Noise Ratio (SINR) [4, 5]:

(4) $$\mathrm{SINR} = \frac{\sigma_{\mathrm{s}}^2 \left| W^{\mathrm{H}} a_{\mathrm{c}} \right|^2}{W^{\mathrm{H}} K_{\mathrm{j+n}} W}\,,$$

where $K_{\mathrm{j+n}}$ is the "interference + noise" covariance matrix of size $M \times M$, and σ_{s}^2 is the signal power. The easy solution can be found by maintaining a distortionless response toward signal and minimizing the power at the filter output. This method is based on the linear constrained optimization. The criterion of optimization is formulated as

(5) $$\min_{W} W^{\mathrm{H}} K_{\mathrm{j+m+n}} W \quad \text{subject to } W^{\mathrm{H}} a_{\mathrm{c}} = 1\,.$$

The solution of the optimization problem (5) is known as the Minimum Variance Distortionless Response beamformer (MVDR) with the weights calculated as

(6) $$W_{\mathrm{MVDR}} = \frac{K_{\mathrm{j+n}}^{-1} a_{\mathrm{c}}}{a_{\mathrm{c}}^{\mathrm{H}} K_{\mathrm{j+n}}^{-1} a_{\mathrm{c}}}\,.$$

In real practical applications, the sample covariance matrix $\widehat{K}$ is used instead of $K_{\mathrm{j+n}}$, which is unavailable. The sample covariance matrix is estimated as

(7) $$\widehat{K} = \frac{1}{N} \sum_{n=1}^{N} x(n) x^{\mathrm{H}}(n)\,.$$

Taking into account this equation the expression for calculating the weights takes the form

(8) $$\widehat{W}_{\mathrm{MVDR}} = \frac{\widehat{K}^{-1} a_{\mathrm{c}}}{a_{\mathrm{c}}^{\mathrm{H}} \widehat{K}^{-1} a_{\mathrm{c}}}\,.$$

Many practical applications of the MVDR-beamforming require online calculation of the weights according to (8), and it means that the covariance matrix (7) should be estimated and inverted online. However, this operation is very expensive computationally and it may be difficult to estimate the sample covariance matrix in real time if the number of samples is large. Furthermore, the numerical calculation of the weights W_{MVDR}, using expression (8) may be very unstable if the sample covariance matrix is ill-conditioned. A numerical stable and computationally efficient algorithm can be obtained by using QR-decomposition of the incoming signal matrix. The signal matrix is decomposed as $X=QR$, where Q is the unitary matrix and R is the upper triangular matrix. Hence the QR-based algorithm for calculation of the beamformer weights includes the following three stages:

- The linear equation system $R^{\mathrm{H}} z_1 = a_{\mathrm{c}}$ is solved for z_1, and the solution is
$$z_1^* = (R^{\mathrm{H}})^{-1} a_{\mathrm{c}} .$$
- The linear equation system $R z_2 = z_1^*$ is solved for z_2, and the solution is
$$z_2^* = R^{-1} z_1^* .$$
- The weight vector $\widehat{W}$ is obtained as $\widehat{W} = z_2^* / (a_{\mathrm{c}}^{\mathrm{H}} z_2^*)$.

5. Array configuration

Antenna arrays are composed of many antennas working in concert to establish an unique radiation pattern in the desire direction. The antenna elements are put together in a known geometry, which is usually uniform – Uniform Linear Arrays (ULA), Uniform Rectangular Arrays (URA) or Uniform Circular Arrays (UCA) [6, 7]. The ULA beam pattern can be controlled only in one dimension, while a URA or a UCA with the elements extended in two dimensions enable to control the beam pattern in two dimensions.

ULA configuration. In ULA configurations, all elements are aligned along a straight line and generally have a uniform interelement spacing d. The direction of a signal arriving from azimuth φ can be described with a unit vector e in Cartesian coordinates, which is pointed from the array element towards the signal wave front. As shown in Fig. 1, azimuth φ is defined to be the angle between the Y-axis and the signal direction of arrival.

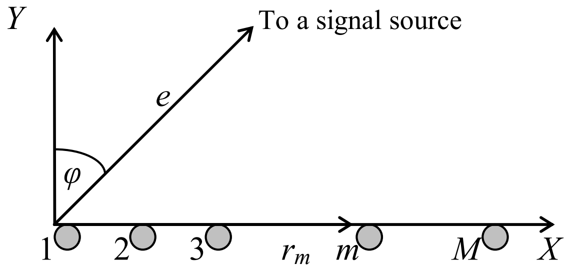

Fig. 1. ULA configuration

The direction unit vector e in Cartesian coordinates can be written as

(9) $$e(\varphi) = (e_X, e_Y) = (\sin\varphi, \cos\varphi) .$$

The vector in the direction of element m can be written in Cartesian coordinates as

(10) $$\vec{r}_m = (d(m-1),\ 0)\,.$$

If the first element of the M-element linear array serves as a reference element, the propagation path-length difference d_m for a signal incident at element m can be defined as the projection of the vector r_m on the direction unit vector e:

(11) $$d_m = e^{\mathrm{T}} \cdot r_m = d \sin\varphi (m-1)\,.$$

Compared to the reference element, the signal incident at array element m from azimuth φ can be expressed as

(12) $$x_m(t) = s(t)\exp\left(j\frac{2\pi}{\lambda} d_m \right) \text{ for } m=1,\ \ldots,\ M,$$

where $s(t)$ is the signal incident at the reference array element. Using the vector notation, the signal incident at the antenna array gives a signal vector with M elements:

(13) $$X(t,\varphi) = s(t)\left[1,\ \exp\left(j\frac{2\pi}{\lambda} d_2 \right), \ldots,\ \exp\left(j\frac{2\pi}{\lambda} d_m \right), \ldots,\ \exp\left(j\frac{2\pi}{\lambda} d_M \right) \right].$$

Therefore, the ULA response vector a_{c} takes the form:

(14) $$a_{\mathrm{c}}(\varphi) = \left[1,\ \exp\left(j\frac{2\pi}{\lambda} d_2 \right), \ldots,\ \exp\left(j\frac{2\pi}{\lambda} d_m \right), \ldots,\ \exp\left(j\frac{2\pi}{\lambda} d_M \right) \right].$$

URA configuration. In URA configurations, all elements are extended in the X-Y plane. There are M_X elements in X-direction and M_Y elements in Y-direction, creating an array of $M_X \times M_Y$ elements. All elements are uniformly spaced d apart in both directions. Such a rectangular array can be viewed as M_Y uniform linear arrays of M_X elements or M_X uniform linear arrays of M_Y elements. Usually, the first antenna element is considered as the origin of Cartesian coordinates (Fig. 2).

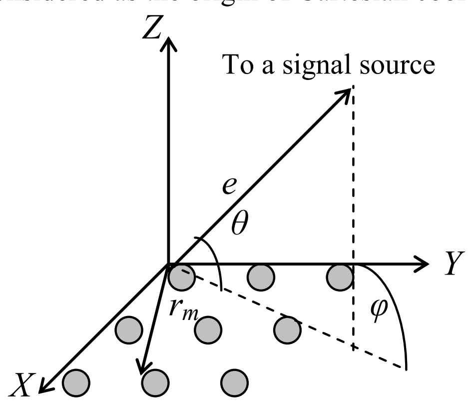

Fig. 2. URA configuration

The direction of a signal arriving from azimuth φ and elevation θ can be described with a unit vector e in Cartesian coordinates as

(15) $$e(\varphi,\ \theta) = (e_X,\ e_Y,\ e_Z) = (\cos\theta\sin\varphi,\ \cos\theta\cos\varphi,\ \sin\theta).$$

The vector in the direction of element $m(i, k)$ can be described in Cartesian coordinates as

(16) $$r_{m(i,k)} = (d(i-1),\ d(k-1),\ 0).$$

Here, i and k denote the element position along the Y- and the X-axis, respectively. The element number $m(i, k)$ is defined as

(17) $$m(i,k) = (i-1)M_X + k, \quad i = 1, ..., M_Y,\ k = 1, ..., M_X.$$

If the first element of the rectangular array serves as a reference element, the path-length difference $d_{m(i,\ k)}$ for a signal incident at element with the sequential number $m(i, k)$ can be defined as the projection of the vector $r_{m(i,\ k)}$ on the signal direction vector e:

(18) $$d_{m(i,k)} = e^{\mathrm{T}} \cdot r_{m(i,k)} = \cos\theta \cdot d[\sin\varphi(i-1) + \cos\varphi(k-1)].$$

Therefore, the signal incident at the antenna array can be written as M-element vector:

(19) $$X(t,\ \varphi,\ \theta) = s(t)\left[1, \exp\left(j\frac{2\pi}{\lambda}d_2\right), \ldots, \exp\left(j\frac{2\pi}{\lambda}d_{m(i,k)}\right), \ldots, \exp\left(j\frac{2\pi}{\lambda}d_M\right)\right],$$

where $M = M_X \times M_Y$. The array response vector a_c takes the form

(20) $$a_c(\varphi,\ \theta) = \left[1,\ \exp\left(j\frac{2\pi}{\lambda}d_2\right), \ldots, \exp\left(j\frac{2\pi}{\lambda}d_{m(i,k)}\right), \ldots, \exp\left(j\frac{2\pi}{\lambda}d_M\right)\right].$$

UCA configuration In UCA configurations, all elements are arranged along the ring of radius r (Fig. 3). The ring contains M array elements.

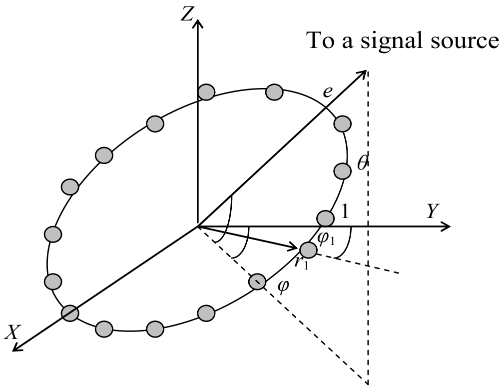

Fig. 3. UCA configuration

Since these elements are uniformly spaced within the ring, so they have an interelement angular spacing $\Delta\varphi = 2\pi/M$, and a linear interelement spacing $d = 2r\pi/M$. It is usually assumed that the first antenna element is located at the Y-axis, and the ring center serves as the origin of Cartesian coordinates. The vector in the direction of element m can be written in Cartesian coordinates as:

(21) $$r_m = (r\sin\varphi_m, r\cos\varphi_m, 0), \quad \text{where } \varphi_m = 2\pi(m-1)/M.$$

The unit vector $e(\varphi,\ \theta)$ in the direction of a signal source is the same as in the URA case. If the center of the ring serves as a reference point, the propagation path-length difference d_m for a signal incident at element m can be defined as the projection of the vector r_m on the direction vector e:

(22)
$$d_m = e^{\mathrm{T}} r_m = d\cos\theta(\sin\varphi\sin\varphi_m + \cos\varphi\cos\varphi_m) = \\ = d\cos\theta\cos(\varphi - \varphi_m).$$

The signal incident at the circular antenna array can be written as M-element vector:

(23)
$$X(t,\ \varphi,\ \theta) = s(t)\left[\exp\left(j\frac{2\pi}{\lambda}d_1\right),\ \exp\left(j\frac{2\pi}{\lambda}d_2\right),\ldots,\ \exp\left(j\frac{2\pi}{\lambda}d_M\right)\right].$$

The array response vector a_{c} takes the form

(24)
$$a_{\mathrm{c}}(\varphi,\ \theta) = \left[\exp\left(j\frac{2\pi}{\lambda}d_1\right),\ \exp\left(j\frac{2\pi}{\lambda}d_2\right),\ldots,\ \exp\left(j\frac{2\pi}{\lambda}d_M\right)\right],$$

where d_m is defined above for $m = 1, 2,\ldots, M$.

6. Simulation results

In this section the computer simulation is performed in order to demonstrate the capability of the two beamforming techniques, conventional and MVDR, to separate the incoming signals arrived from different azimuth directions. Each beamforming technique is evaluated in terms of the following parameters:

- *The Half Power Beamwidth (HPBW)* is the angular separation in which the magnitude of the radiation pattern decreases by 50% (or −3 dB) from the peak of the main beam. This measure determines the minimal difference between the Directions-Of-Arrival (DOA) of the two signals that can be separated by the beamforming technique $\Delta\varphi$;
- *The Peak Sidelobe Level (PSL)* is the radiation in an undesired direction which can never be completely eliminated;
- *The Improvement in the Signal-to-Interference-plus-Noise* ratio is the *Ratio* between SINR at the single array element and SINR at the beamformer output (*IMP*).

Two scenarios have been used in computer simulations.

Scenario 1 – Single desired signal

According to this scenario, the received signal consists of a single PRN coded signal arriving from a source with the angular coordinates: 30° (azimuth) and 5° (elevation). The carrier frequency is 1.251 MHz, the sampling frequency is 5.005 MHz, the frequency bandwidth is 2 MHz and the signal duration is 1 ms. For comparison analysis we selected three different array configurations, ULA, URA and UCA, with 9 elements. The numerical results obtained for both beamforming techniques in case when only the receiver noise corrupts the desired signal are presented in Table 1. In that case the input Signal-to-Noise Ratio (SNR) at a single array element varies from 0 to 20 dB. It can be seen that the azimuth resolution ($\Delta\varphi$) of the MVDR method betters with the increase of SNR very much. For a conventional beamformer, the azimuth resolution improves poorly with the increase of SNR. The analysis of the results summarized in Table 1 shows that the best azimuth resolution is achieved by the ULA configuration. As to the peak side lobe level, for the conventional method, the PSL slowly decreases with increase of SNR. However, for the MVDR method, the peak sidelobe level is drastically down from –7 to –26 dB, when SNR increases from 0 to 20 dB. In the interference-free case both methods improve SNR by 6 dB.

The numerical results obtained for the case when the jammer disturbs the reception of the desired signal are presented in Table 2. The jammer direction has the angular coordinates: azimuth of –60° and elevation of –5°. The jamming intensity is determined by the Interference-to-Signal-Ratio (ISR). The results presented in Table 2 are obtained for the case when SNR is 10 dB, and the ISR varies in the range of 0 to 20 dB. The analysis of the results shows that the MVDR method retains the important characteristics such as azimuth resolution and sidelobes, over a wide range of interference intensity. It is so because the MVDR succeeds entirely to suppress interference. This view is substantiated by the growth of IMP with increase of ISR. Unfortunately, this is not true for the conventional beamforming method. Its characteristics are degraded very much when the interference intensity increases.

Table 1. Performance measures for an interference-free environment

Array	SNR, dB	Conventional BF			MVDR BF		
		$\Delta\varphi$,°	PSL, dB	IMP, dB	$\Delta\varphi$,°	PSL, dB	IMP, dB
ULA	0	15.4	–6.5	6.5	8.10	–7.2	6.5
	5	14.1	–9.4	6.5	4.50	–11.5	6.5
	10	**13.6**	**–11.4**	**6.5**	**2.20**	**–16.3**	**6.2**
	20	13.4	–12.8	6.5	0.84	–26.3	4.7
URA	0	42.6	–5.6	6.5	22.5	–6.9	6.5
	5	38.4	–7.7	6.5	12.3	–11.3	6.5
	10	**36.9**	**–8.8**	**6.5**	**6.7**	**–16.0**	**6.2**
	20	36.6	–9.5	6.5	1.8	–26.0	4.7
UCA	0	47.6	–5.0	6.5	26.1	–6.8	6.4
	5	43.1	–6.6	6.5	13.9	–11.1	6.4
	10	**42.0**	**–7.5**	**6.5**	**7.9**	**–15.8**	**6.4**
	20	41.4	–7.8	6.5	2.1	–25.8	4.2

Table2. Performance measures for an interference environment

Array	ISR, dB	Conventional BF			MVDR BF		
		$\Delta\varphi$,°	PSL, dB	IMP, dB	$\Delta\varphi$,°	PSL, dB	IMP, dB
ULA	0	13.8	–11.1	15.7	2.2	–16.3	16.6
	5	**13.9**	**–10.4**	**18.5**	**2.2**	**–16.3**	**21.4**
	10	14.3	–8.8	20.4	2.2	–16.3	26.4
	20	22.2	–3.5	21.4	2.2	–16.3	36.2
URA	0	37.1	–8.8	16.6	7.6	–15.8	16.7
	5	**37.3**	**–8.6**	**20.6**	**7.6**	**–15.8**	**21.2**
	10	37.8	–8.3	23.8	7.6	–15.8	26.1
	20	42.1	–5.7	26.7	7.6	–15.8	35.7
UCA	0	48.4	–4.9	6.4	8.1	–15.8	16.2
	5	**65.6**	**–2.8**	**6.4**	**8.1**	**–15.8**	**20.8**
	10	–	–1.2	6.4	8.1	–15.8	25.8
	20	–	0	6.4	8.1	–15.8	35.7

Scenario 2 – Two desired signals

According to this scenario the received signal consists of two desired signals arriving from two close directions. The source angular coordinates are selected for each array configuration in accordance with the results from Table 2, for ISR = 5 dB. The directions of arrival of the two signals are presented in Table 3.

Table 3. Signal directions for Scenario 2

Array	Signal 1		Signal 2	
	Azimuth (φ,°)	Elevation (θ,°)	Azimuth (φ,°)	Elevation (θ,°)
ULA	28.5	5	31.5	5
URA	26.3	5	33.7	5
UCA	26	5	34	5

In order to compare the capability of the two beamformers to separate two signals arriving from close azimuth directions, the normalized output power of each beamformer is calculated by varying the azimuth in range of –90° to 90° for SNR =10 dB and ISR = 5 dB. The signal power at the output of the two beamformers is presented in Fig. 4 – for the ULA, in Fig. 5 – for the URA and in Fig. 6 – for the UCA.

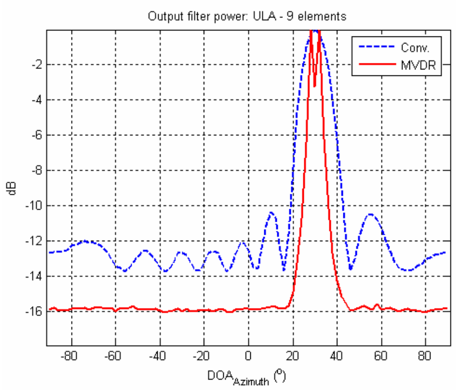

Fig. 4. Signal azimuth separation by the ULA

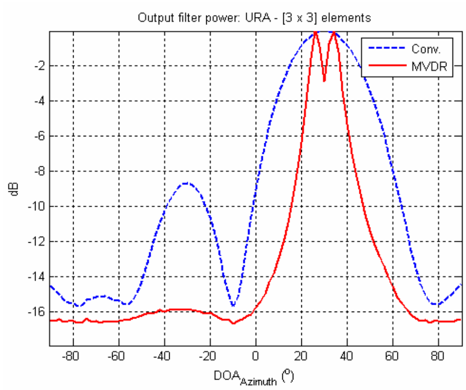

Fig. 5. Signal azimuth separation by the URA

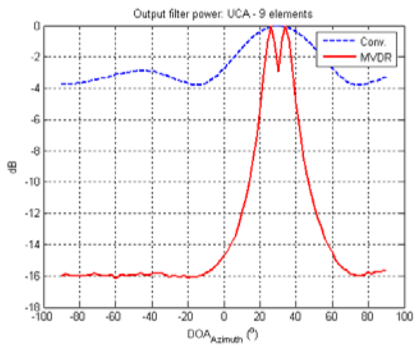

Fig. 6. Signal azimuth separation by the UCA

The graphical results demonstrate the capability of the beamforming methods to separate signals with small arrival-azimuth diversity. It can be seen that the plotted results prove the values of the azimuth resolution presented in Table 2.

7. Conclusions

In this paper, the performance of the two beamforming methods, conventional and MVDR, is simulated for three array configurations and different jamming/noise intensities. The simulation results demonstrate the better and stable resolution and the better accommodation capability of the MVDR method compared to the conventional method.

Acknowledgment. This work is partially supported by the National Science Fund (Project MI-1506/05 and Project MU-FS-05/2007).

References

1. Godara, L. Application of Antenna Arrays to Mobile Communications. Part II: Beam-Forming and Direction-of-Arrival Considerations. – In: Proc. of the IEEE, Vol. **85**, 1997, No 8, 1195-1245.
2. Trees, H., L. Van. Optimum Array Processing. Part IV. Detection, Estimation, and Modulation Theory. New York, NY: JohnWiley and Sons, Inc., 2002.
3. Fu, Z., A. Hombostel, J. Hammesfahr, A. Konovaltsev. Suppression of Multipath and Jamming Signals by GPS/Galileo Applications. – GPS Solutions, 2003, No 6, 257-264.
4. Tummonery, L., I. Proudler, A. Farina, J. McWhirter. QRD-Based MVDR Algorithm for Adaptive Multi-Pulse Antenna Array Signal Processing. – In: Proc. Radar, Sonar, Navigation, Vol. **141**, 1994, No 2, 93-102.
5. Vouras, P., B. Freburger. Application of Adaptive Beamforming Techniques to HF Radar. – In: Proc. IEEE Conf. RADAR'08, May, 2008, p. 6.
6. Moelker, D., E. Van der Pol. Adaptive Antenna Arrays for Interference Cancellation in GPS and GLONASS Receivers. – In: Proc. IEEE 1996 Position Location and Navigation Symp., April 1996, 191-196.
7. Ioannides, P., C. A. Balanis. Uniform Circular and Rectangular Arrays for Adaptive Beamforming Applications. – In: IEEE Trans. Antenn. Wireless Propagat. Lett., Vol. **4**, 2005, 351-354.